Journal of Physics: Conference Series **133** (2008) 012005 doi:10.1088/1742-6596/133/1/012005

A multi term Boltzmann equation analysis of non-conservative electron transport in time-dependent electric and magnetic fields

S Dujko[1,2] and R D White[2]

[1] Institute of Physics, University of Belgrade, PO BOX 68, 11080 Zemun, Belgrade, Serbia
[2] ARC Centre for Antimatter-Matter Studies, School of Mathematics, Physics and IT, James Cook University, Townsville 4811, QLD, Australia

E-mail: sasa.dujko@jcu.edu.au

Abstract. A multi term technique for solving the Boltzmann equation has been developed to investigate the time-dependent behavior of charged particle swarms in an unbounded neutral gas under the influence of spatially uniform time-dependent electric and magnetic fields. The hierarchy resulting from a spherical harmonic decomposition of the Boltzmann equation in the hydrodynamic regime is solved numerically by representing the speed dependence of the phase-space distribution function in terms of an expansion in Sonine polynomials about a Maxwellian velocity distribution at an internally determined time-dependent temperature. This technique avoids restrictions on the electric and magnetic field amplitudes and frequencies and/or the charged particle to neutral molecule mass ratio traditionally associated with many investigations. The variation of the electron transport coefficients with electric and magnetic field strengths, field frequency, phase difference between the fields and angle between the fields is addressed using physical arguments for certain model and real gases.

1. Introduction

In recent years interest in charged particle transport processes in neutral gases under the conditions of ac electric and magnetic fields has been revived. This interest was motivated by the desire to understand the physics underlying the operation of magnetically controlled/assisted ac plasma discharges in which magnetic field affects both the electron heating mechanisms and charged particle species transport. Large classes of non-equilibrium plasma devices utilize electromagnets, permanent magnets or induced magnetic fields with the goal of enhancing plasma density or improving electron confinement [1]. Hence one of the most challenging areas in plasma modeling is an accurate representation of the effects of a magnetic field on charged particle kinetics.

The history with respect to various aspects of charged particle transport processes in electric and magnetic fields and techniques for solving the Boltzmann equation has been recently reviewed [2, 3]. In contrast to the extensive literature on charged particle swarms in dc electric and magnetic fields, until recently very little has been carried over to charged particle swarms in ac electric and magnetic fields. In order to achieve this goal, a general and accurate theory is required. Such a theory, in ac electric and magnetic fields crossed at arbitrary angle based on the spherical harmonics decomposition of the Boltzmann equation has been published by White

et al [2]. In this paper we make a further generalization of the theory with respect to the work of White *et al* [2] to consider the explicit effects of non-conservative collisions.

We begin this paper with a brief review of a multi term theory for solving the Boltzmann equation valid for both electrons and ions in time-dependent electric and magnetic fields crossed at arbitrary angles, incorporating the effects of non-conservative collisional processes. We focus on the time-dependent behavior of electron transport properties under conditions which can be generally found in magnetically controlled/assisted rf discharges. We systematically investigate the explicit effects associated with the electric and magnetic fields including field to density ratios, field frequency, field phases and field orientations. In addition we will highlight the explicit modification of transport coefficients by non-conservative collisional processes of attachment and ionization. A multitude of kinetic phenomena were observed that are generally inexplicable through the use of steady-state dc transport theory. We systematically study the origin and mechanisms for such phenomena, their sometimes paradoxical manifestation and possible physical implications which arise from their explicit inclusion into plasma models.

2. Theory

The behavior of charged particles in gases under the influence of electric and magnetic fields is described by the phase-space distribution function $f(\boldsymbol{r}, \boldsymbol{c}, t)$ representing the solution of the Boltzmann equation

$$\frac{\partial f}{\partial t} + \boldsymbol{c} \cdot \frac{\partial f}{\partial \boldsymbol{r}} + \frac{q}{m} \left[\boldsymbol{E}(t) + \boldsymbol{c} \times \boldsymbol{B}(t)\right] \cdot \frac{\partial f}{\partial \boldsymbol{c}} = -J\left(f, f_0\right) . \tag{1}$$

Here r and c denote the position and velocity co-ordinates, q and m are the charge and mass of the swarm particle, t is time while E and B are magnitudes of the electric and magnetic fields, respectively. In what follows, we employ a co-ordinate system in which $\boldsymbol{E}$ defines the z-axis while $\boldsymbol{B}$ lies in the y-z plane, making an angle ψ with respect to the $\boldsymbol{E}$. The right-hand side of Eq. (1) denotes the linear charged particle-neutral molecule collision operator, accounting for elastic, inelastic and nonconservative (e.g. ionizing and attaching) collisions. For elastic collisions we use the original Boltzmann collision operator [4], while for inelastic collisions we prefer the semiclassical generalization of Wang-Chang et al. [5]. The attachment and ionization collision operators employed are detailed in Ref. [6].

Swarm conditions are assumed to apply where the charged particle number density is much less than number density of neutral species and mutual interactions between swarm particles are negligible compared with swarm particle-neutral particle interactions. We assume the neutral molecules (of number density n_0) remain in thermal equilibrium at a temperature T_0 and their internal states are characterized by a Boltzmann distribution. No space charge fields are considered and both the electric and magnetic fields are spatially homogeneous and time-dependent.

2.1. Time-dependent hydrodynamic regime and definition of transport coefficients

The connection between experimental and theoretical investigations of swarm behavior is usually made through the equation of continuity

$$\frac{\partial n(\boldsymbol{r}, t)}{\partial t} + \nabla \cdot \boldsymbol{\Gamma}(\boldsymbol{r}, t) = S(\boldsymbol{r}, t) , \tag{2}$$

where

$$n(\boldsymbol{r}, t) = \int f(\boldsymbol{r}, \boldsymbol{c}, t) \mathrm{d}t , \tag{3}$$

while $\boldsymbol{\Gamma}(\boldsymbol{r}, t) = n\langle \boldsymbol{c} \rangle$ is the swarm particle flux and $S(\boldsymbol{r}, t)$ represents the production rate per unit volume per unit time arising from non-conservative collisional processes.

Far from boundaries,sources and sinks, the hydrodynamic regime is assumed to apply. In the time-dependent hydrodynamic regime the space-time dependence is entirely carried out by the density $n(\boldsymbol{r},t)$ of charged particles and the distribution function has the form

$$f(\boldsymbol{r},\boldsymbol{c},t)=\sum_{k=0}^{\infty} f^{(k)}(\boldsymbol{c},t)\odot(-\nabla)^k\, n(\boldsymbol{r},t)\,, \tag{4}$$

where $f^{(k)}(\boldsymbol{c},t)$ are time-dependent tensors of rank k and $\odot$ denotes a k-fold scalar product.

Assuming the functional relationship (4), the flux $\boldsymbol{\Gamma}(\boldsymbol{r},t)$ and source term $\boldsymbol{S}(\boldsymbol{r},t)$ in (2) are expanded as follows:

$$\boldsymbol{\Gamma}(\boldsymbol{r},t)=\boldsymbol{W}^{\star}(t)n(\boldsymbol{r},t)-\boldsymbol{D}^{\star}(t)\cdot\nabla n(\boldsymbol{r},t)\,, \tag{5}$$

$$S(\boldsymbol{r},t)=S^{(0)}(t)n(\boldsymbol{r},t)-\boldsymbol{S}^{(1)}(t)\cdot\nabla n(\boldsymbol{r},t)+\boldsymbol{S}^{(2)}(t):\nabla\nabla n(\boldsymbol{r},t) \tag{6}$$

where $\boldsymbol{W}^{\star}(t)$ and $\boldsymbol{D}^{\star}(t)$ define, respectively, the *flux* drift velocity and *flux* diffusion tensor. Substitution of expansion (5) and (6) into the continuity equation (2) yields the time-dependent diffusion equation,

$$\frac{\partial n(\boldsymbol{r},t)}{\partial t}+\boldsymbol{W}(t)\cdot\nabla n-\boldsymbol{D}(t):\nabla\nabla n=-R_a(t)n\,, \tag{7}$$

which define the *bulk* transport coefficients

$$R_a=-S^{(0)} \qquad \text{(loss rate)}\,, \tag{8}$$

$$\boldsymbol{W}=\boldsymbol{W}^{(\star)}+\boldsymbol{S}^{(1)} \qquad \text{(bulk drift velocity)}\,, \tag{9}$$

$$\boldsymbol{D}=\boldsymbol{D}^{(\star)}+\boldsymbol{S}^{(2)} \qquad \text{(bulk diffusion tensor)}\,. \tag{10}$$

In swarm experiments the bulk transport coefficients are generally measured and tabulated. These transport coefficients are associated with the swarms centre of mass transport. The explicit influence of non-conservative collisional processes on the swarms centre of mass transport is described by the correction terms $S^{(1)}$ and $S^{(2)}$. Obviously, in the absence of non-conservative processes, these two sets of transport coefficients coincide. The distinction between these two sets of transport coefficients was discussed at length in the 1980s, but has been ignored in the majority of previous work in the plasma modeling community. This has lead to a potentially serious mismatch between input swarm data (generally the bulk transport properties) and the parameters (often the flux transport properties) required in many plasma fluid models [9]. Note that only theory, i.e. Boltzmann equation calculations and/or Monte Carlo simulations, can resolve any such mismatch, by providing both flux and bulk transport coefficients.

2.2. Spherical harmonics decomposition of the Boltzmann equation

The angular dependence of the phase-space distribution function in velocity space can be represented in terms of an expansion in spherical harmonics:

$$f(\boldsymbol{r},\boldsymbol{c},t)=\sum_{l=0}^{\infty}\sum_{m=-l}^{l} f_m^{(l)}(\boldsymbol{r},c,t)Y_m^{[l]}(\hat{\boldsymbol{c}})\,, \tag{11}$$

where $Y_m^{[l]}(\hat{\boldsymbol{c}})$ are spherical harmonics and $\hat{\boldsymbol{c}}$ denotes the angles of $\boldsymbol{c}$. The value of l is incremented until some predefined accuracy criterion is satisfied. This value indicates the deviation of the velocity distribution function from isotropy.

Assuming the time-dependent hydrodynamic regime, the spatial dependence is represented by

$$f_m^{(l)}(\boldsymbol{r},c,t)=\sum_{s=0}^{\infty}\sum_{\lambda=0}^{s}\sum_{\mu=-\lambda}^{\lambda} f(lm|s\lambda\mu;c,t)G_\mu^{(s\lambda)}n(\boldsymbol{r},t)\,, \tag{12}$$

where $G_\mu^{(s\lambda)}$ is the irreducible gradient operator [6]. Truncation at $s=2$ is necessary to determine transport coefficients up to and including diffusion when non-conservative collisions are operative.

The speed dependence of the coefficients in Eq. (12) is represented by an expansion about a Maxwellian at an arbitrary time-dependent temperature $T_b(t)$, in terms of Sonine polynomials

$$f(lm|s\lambda\mu;c,t)=\omega(\alpha(t),t)\sum_{\nu=0}^{\infty}F(\nu lm|s\lambda\mu;\alpha(t),t)R_{\nu l}(\alpha(t)c)\,, \tag{13}$$

where

$$R_{\nu l}(\alpha(t)c)=N_{\nu l}\left[\frac{\alpha(t)c}{\sqrt{2}}\right]^l S_{l+1/2}^{(\nu)}\left(\frac{\alpha^2(t)c}{2}\right)\,, \tag{14}$$

$$\omega(\alpha(t),c)=\left[\frac{\alpha^2(t)}{2\pi}\right]^{3/2}\exp\left[-\frac{\alpha^2(t)c^2}{2}\right]\,, \tag{15}$$

$$\alpha^2(t)=\frac{m}{kT_b(t)}\,, \tag{16}$$

$$N_{\nu l}^2=\frac{2\pi^{3/2}\nu!}{\Gamma(\nu+l+3/2)}\,, \tag{17}$$

and $S_{l+1/2}^{(\nu)}\left(\frac{\alpha^2(t)c}{2}\right)$ are Sonine polynomials. Using the appropriate orthogonality relations of the spherical harmonics and modified Sonine polynomials the following system of coupled differential equations for the moments $F(\nu lm|s\lambda\mu;\alpha(t),t)$ is generated:

$$\sum_{\nu'=0}^{\infty}\sum_{l'=0}^{\infty}\sum_{m'=-l'}^{l'}\Bigg\{\partial_t\delta_{\nu\nu'}\delta_{ll'}\delta_{mm'}+\omega(000;t)\delta_{\nu\nu'}\delta_{ll'}\delta_{mm'}+n_0J_{\nu\nu'}^l\delta_{ll'}\delta_{mm'}$$

$$+ia(t)(l'm10|lm)\alpha(t)<\nu l||K^{[1]}||\nu'l'>\delta_{mm'}$$

$$+\frac{q}{m}B(t)\Bigg\{\frac{\sin\psi}{2}\Big[\sqrt{(l-m)(l+m+1)}\delta_{m'm+1}-\sqrt{(l+m)(l-m+1)}\delta_{m'm-1}$$

$$-im\cos\psi\delta_{mm'}\Big]\Bigg\}\delta_{\nu\nu'}\delta_{ll'}\Bigg\}F(\nu'l'm'|s\lambda\mu;\alpha(t),t)=X(\nu lm|s\lambda\nu;\alpha(t),t)\,, \tag{18}$$

where $J_{\nu\nu'}^l$ and $\langle\nu l||K^{[1]}\nu'l'\rangle$ are reduced matrix elements, $\omega(000)$ represents the net creation rate and $(lm|l'm10)$ is a Clebsch-Gordan coefficient. The explicit expressions for the RHS are given in Ref. [7]. Discretising in time using an implicit finite difference scheme converts the system of coupled differential equations into a hierarchy of coupled complex equations. This sparse system of equations is solved using standard sparse inversion routines. The explicit expressions for both bulk and flux transport coefficients including the mean energy, gradient energy vector components and temperature tensor components are given in Refs. [2, 7].

3. Results and discussion

3.1. Preliminaries

In this section we consider the electron transport in rf electric and magnetic fields under hydrodynamic conditions using a multi term theory for solving the Boltzmann equation. Similar studies have been published previously for the Reid ramp model in a crossed field configuration [2, 3]. We try to complement these previous publications by a comprehensive description of electron transport for the most general case of arbitrary field orientations and phase differences between the fields. In addition, in this paper we make a further generalization with respect to the work of White *et al* [2] to consider the explicit effects associated with non-conservative collisions. The ionization model of Lucas and Saelee [8] is employed in this work with the goal of understanding the effects of the ionization processes. Another important aspect of this work is that we investigate the influence of varying field frequency and phase difference between the fields on the electron transport properties in carbon tetrafluoride (CF_4). CF_4 provides an example of a gas which has applications in a wide range of devices where the electron kinetics plays an important role in device behavior. For example, CF_4 has application in rf plasmas mostly realized in capacitively coupled plasma (CCP) [10] and even in ICP for silicon etching [11]. The knowledge of electron transport coefficients and in particular the values of electric and magnetic field strengths for which non-conservative collisions (attachment/ionization) may or may not have a significant effect on the drift and diffusion properties may be important for the operation of these devices. We employ a set of cross sections for CF_4 developed by Kurihara *et al* [12]. For illustrative purposes we chose an applied electric field of 100 Td (1Td $= 10^{-21}$ Vm^{-2}) to ensure the average energy of the swarm is in the range where some interesting kinetic phenomena may be induced. The theory and associated code have been benchmarked against an independent time-resolved Monte Carlo simulation [13].

3.2. The effects of the magnetic field strength

In this section we investigate the influence of the magnetic field strength on the electron transport properties in CF_4. In Figure 1, we display the temporal profiles of the (a) mean energy, (b) longitudinal and (c) transverse drift velocity components and (d) diffusion coefficient along the $\boldsymbol{E}\times\boldsymbol{B}$ direction, as a function of B_0/n_0 in a crossed field configuration for a fixed phase difference of $\pi/3$ rad between the fields. The mean energy is decreased for an increasing B_0/n_0. We may observe that the symmetric profile of the mean energy for the magnetic field free case becomes asymmetric and triangular at high B_0/n_0 with a fast increase and slower decrease.

Both components of the drift velocity lose the symmetry with increasing magnetic field amplitude and at the highest magnetic field strong oscillations are induced due to the cyclotron rotation of the electron swarm. These oscillations represent essentially collision-less gyro-orbits of the swarm particles during this phase of the cycle. Transverse component along $\boldsymbol{E}\times\boldsymbol{B}$ direction is more asymmetric than the longitudinal component, thus resulting in a cycle-averaged value that is non-zero. These figures clearly show how dramatic the influence of the magnetic field can be. The magnetic field and resulting Lorentz force in the $\boldsymbol{E}\times\boldsymbol{B}$ direction produces a macroscopic drift in that direction as well as complex, asymmetric behavior of the longitudinal component of drift velocity.

The transverse diffusion coefficient along the $\boldsymbol{E}\times\boldsymbol{B}$ direction shows some unexpected features. We observe that it has all the features of anomalous diffusion [3] but perhaps the most striking phenomena is the presence of negative transiently diffusivity in the limit of the highest B_0/n_0 of 2000 Hx (1Hx $= 10^{-27}$ Tm^3). These results independently confirm the previous calculations and the reader is referred to [14] for details. Generally speaking, the temporal profiles presented in Fig. 1 (a)-(d) are not predictable from steady-state dc theory. The temporal non-locality in association with the effects of magnetic field result in complex temporal profiles of the electron transport coefficients in rf electric and magnetic fields.

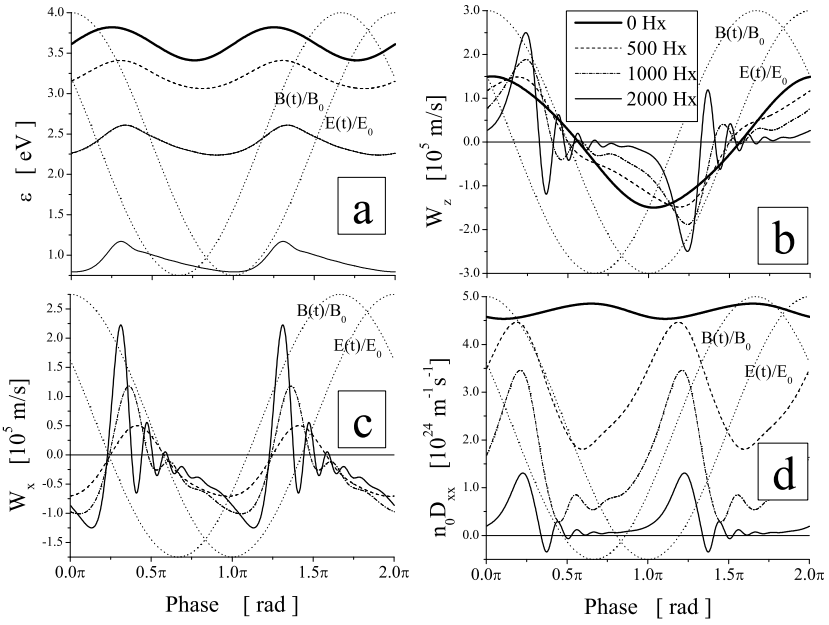

Figure 1. Temporal profiles of (a) mean energy, (b) longitudinal and (c) transverse drift velocity components and (d) diffusion coefficient along the $\boldsymbol{E} \times \boldsymbol{B}$ direction for electrons in CF_4 under the influence of B_0/n_0 for a fixed phase difference of $\pi/3$ rad. The electric field amplitude is set to 100 Td, the field frequency is 100 MHz and $n_0 = 3.54 \times 10^{22}$ m^{-3}.

3.3. The effects of the phase difference and the field orientations

In this section we investigate the influence of varying the phase difference between the fields on the electron transport properties for the ionization model of Lucas and Saelee. In Fig. 2, we display the 3-dimensional plots of the temporal profiles of the mean energy and ionization rate as a function of the phase difference between the fields. In the limit of small phase differences, the magnetic field is large when electric field peaks and electrons cannot gain much energy from the electric field - the magnetic field cools the swarm. Consequently, the mean energy is significantly reduced. As the phase difference increases, the magnetic cooling effects are reduced, particularly in phases where electric field peaks (and magnetic field magnitude is small) and we observe that the modulation amplitude and cycle-averaged value are increased.

In contrast to mean energy, the ionization rate exhibits a specific and unexpected behavior. In the limit of large phase differences the ionization rate is significantly modulated while in the limit of small phase differences this transport quantity is significantly reduced. Note that the mean energy does not follow this trend, which implies that the distribution function (and in particular the tail of the distribution) must be also strongly modulated. Thus the phase difference between the fields has important implications for the efficiency of the ionization processes and other inelastic channels that play vital role in maintaining the plasma.

In Fig. 3 we show the 3-dimensional plots of the temporal profiles of the ionization rate and longitudinal diffusion coefficient as a function of the field orientations. As the angle between the fields increases, both transport quantities monotonically decrease for a fixed phase. While the modulation amplitude of $n_0 D_{zz}$ is increased for an increasing angle between the fields, the ionization rate displays the opposite behavior. In addition, in the limit of perpendicular fields the ionization rate is significantly reduced. One may understand this behavior by considering

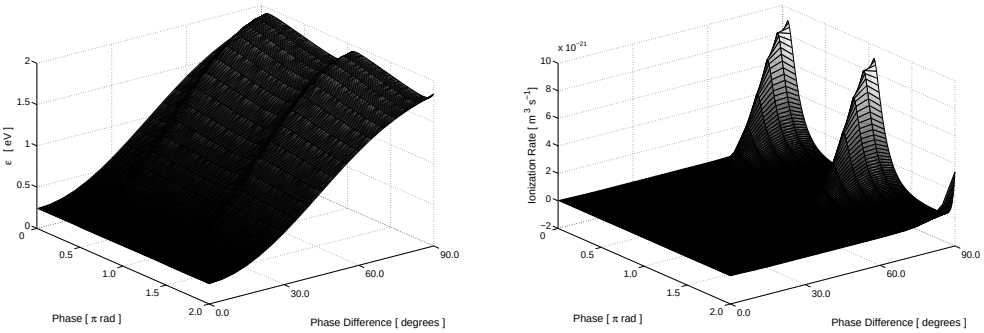

Figure 2. The 3-dimensional plots of the temporal profiles of the mean energy and ionization rate as a function of the phase difference between the fields for the Lucas-Saelee model. The electric and magnetic fields have the following forms $E(t) = 10\cos(\omega t)$ Td and $B(t) = 1000\cos(\omega t + \theta)$ Hx, respectively, where θ is the phase difference while ω/n_0 is the reduced angular frequency of 1×10^{-15} rad m^{-3} s^{-1}.

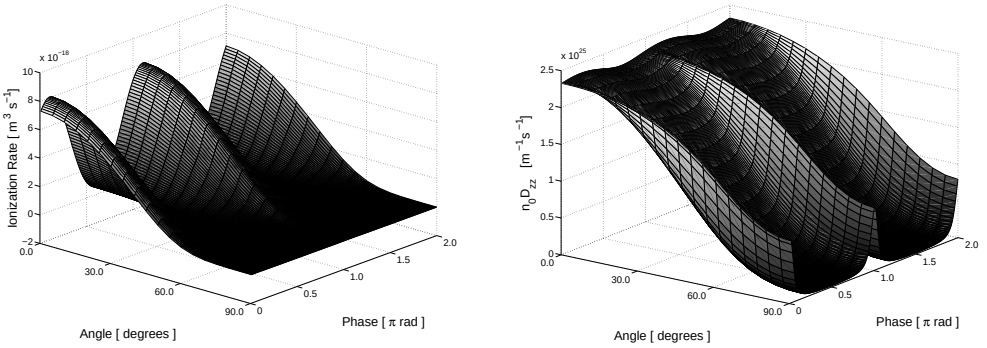

Figure 3. The 3-dimensional plots of the temporal profiles of the mean energy and ionization rate as a function of the angle between the fields for the Lucas-Saelee model. The electric and magnetic fields have the following forms $E(t) = 10\cos(\omega t)$ Td and $B(t) = 1000\sin(\omega t)$ Hx, respectively. The reduced angular frequency ω is set to 1×10^{-15} rad m^{-3} s^{-1}.

the cooling effects associated with the action of an orthogonal component of the magnetic field.

3.4. The effect of the cyclotron resonance on electron transport

One important aspect of this work is that we propose a new additional mechanism for collisional heating in rf electric and magnetic fields caused by the synergism of temporal non-locality and cyclotron resonance effect. The effect of the cyclotron resonance represents the resonant absorption of energy from a radio-frequency or microwave-frequency electromagnetic field by electrons in a uniform dc/rf magnetic field when the frequency of the electromagnetic field equals the cyclotron frequency of the electrons. In Fig. 4 (a) and (b) we demonstrate this effect for the Reid ramp model. The cycle-averaged mean energy is presented as a function of magnetic field amplitude, field frequency and phase difference between the fields. For the field frequency of 50 MHz, the cycle-averaged mean energy is a monotonically decreasing function of magnetic field. However, as the field frequency is increased, the oscillatory-type behavior is clearly evident. The cycle-averaged mean energy is affected by the phase difference between the fields as shown in Fig. 4 (b). For an increasing phase difference, the cycle-averaged mean energy

is increased. These figures clearly show that under specific conditions the magnetic field can efficiently pump the energy into the system. The magnetic field amplitude and field frequency can be tuned to exploit/control this behaviour.

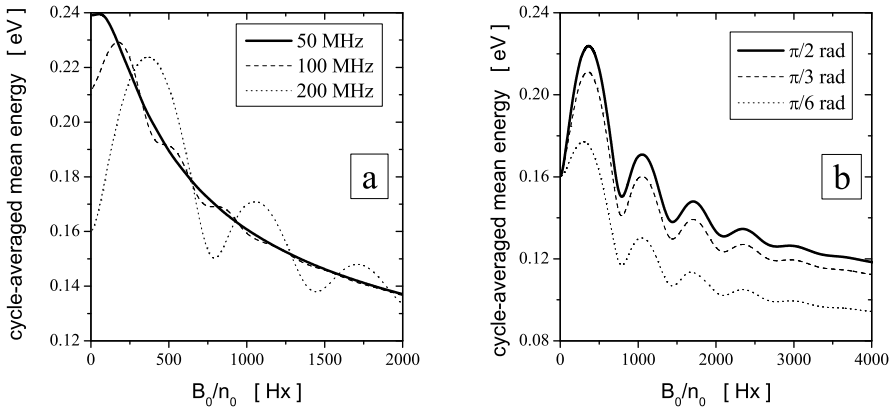

Figure 4. The cycle-averaged mean energy as a function of B/n_0 for various (a) field frequencies, and (b) phase differences for Reid ramp model. The electric field amplitude is set to 14.14 Td, the field frequency is 200 MHz and $n_0 = 3.54 \times 10^{22}$ m^{-3}.

To understand this phenomena we look at the power deposited by the electric field by considering the longitudinal drift velocity shown in Fig. 5. In this figure we can see that increasing magnetic field amplitude decreases the phase delay of the longitudinal drift with respect to the electric field while leaving the drift amplitude relatively unchanged. Consequently the increase in the cycle-averaged mean energy over the range of magnetic field amplitudes 0-400 Hx then follows.

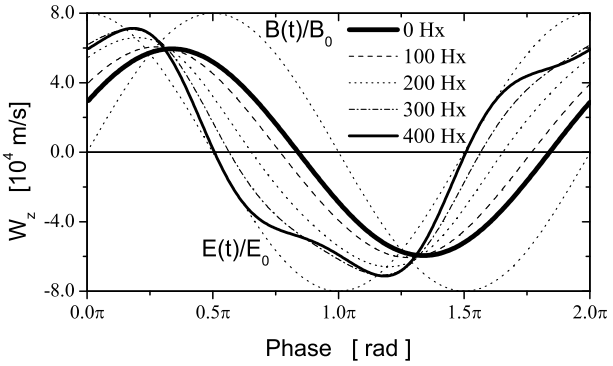

Figure 5. Temporal profiles of the longitudinal drift velocity component as a function of B/n_0 for the Reid ramp model. The electric field amplitude is set to 14.14 Td, the field frequency is 200 MHz and $n_0 = 3.54 \times 10^{22}$ m^{-3}.

4. Conclusion

In this work we have systematically investigated the effects of magnetic field amplitude, field frequency, field orientations and phase difference between the fields on the electron transport properties in rf electric and magnetic fields for a range of model and real gases using a multi term theory for solving the Boltzmann equation. There is a multitude of new phenomena observed which are not predictable from d.c. steady state transport and these results demonstrate the importance of a time-resolved study of electron transport under these conditions. Further to this, and of particular significance in this study, is the ability to suppress/optimize (cycle-averaged) collisional heating under rf electric and magnetic fields through tuning the magnetic field magnitude, frequency and/or phase-difference.

Acknowledgments

The authors would like to thank the support of the Australian Research Council and the Centre for Antimatter-Matter studies. One of the authors (SD) was partly founded by the MNTR project 141025. It is a pleasure to acknowledge helpful discussions with Prof Robert Robson, Dr Kevin Ness and Prof Zoran Petrović.

References

[1] Makabe T and Petrović Z Lj 2006 *Plasma Electronics: Applications in Microelectronic Device Fabrication* (New York: Taylor Francis Group)
[2] White R D, Ness K F and Robson R E 2002 *Appl. Surf. Sci.* **192** 25
[3] Petrović Z Lj, Raspopović Z M, Dujko S and Makabe T 2002 *Appl. Surf. Sci.* **192** 1
[4] Boltzmann L 1872 *Wein. Ber.* **66** 275
[5] Wang-Chang C S, Uhlenbeck G E and DeBoer J 1964 *Studies in Statistical Mechanics* vol 2, ed J DeBoer and G E Uhlenbeck (New York: Wiley) p 241
[6] Robson R E and Ness K F 1986 *Phys. Rev. A* **33** 2068
[7] Dujko S 2008, PhD Thesis, School of Mathematics, Physics and IT, James Cook University
[8] Lucas J and Saelee H T 1975 *J. Phys. D: Appl. Phys.* **8** 640
[9] Robson R E, White R D and Petrović Z Lj 2005 *Rev. Mod. Phys.* **77** 1304
[10] Kitajima T, Takeo T, Petrović Z Lj and Makabe T 2000 *Appl. Phys. Lett* **77** 489
[11] Hioki K, Hirata H, Nakano N, Petrović Z Lj and Makabe T 2000 *J. Vac. Sci. Technol. A* **18** 864
[12] Kurihara M, Petrović Z Lj and Makabe T 2000 *J. Phys. D: Appl. Phys.* **33** 2146
[13] White R D, Dujko S, Ness K F, Robson R E, Raspopović Z Lj and Petrović Z Lj 2007 *Anziam J.* **48** (CTAC2006) C50
[14] White R D, Dujko S, Ness K F, Robson R E, Raspopović Z M and Petrović Z Lj 2008 *J. Phys. D: Appl. Phys.* **41** 025206